PD-1 and LAG-3 inhibitory co-receptors act synergistically to prevent autoimmunity in mice

Taku Okazaki,[1,2,3] Il-mi Okazaki,[1] Jian Wang,[3] Daisuke Sugiura,[1] Fumio Nakaki,[3] Taku Yoshida,[3] Yu Kato,[3] Sidonia Fagarasan,[4] Masamichi Muramatsu,[5] Tomoo Eto,[6] Kyoji Hioki,[6] and Tasuku Honjo[3]

[1]Division of Immune Regulation, Institute for Genome Research, University of Tokushima, Kuramoto, Tokushima 770-8503 Japan
[2]Core Research for Evolutional Science and Technology, Japan Science and Technology Corporation, Tokyo 102-0075, Japan
[3]Department of Immunology and Genomic Medicine, Graduate School of Medicine, Kyoto University, Sakyo-ku, Kyoto 606-8501, Japan
[4]Laboratory of Mucosal Immunity, RIKEN, Tsurumi, Yokohama 230-0045, Japan
[5]Department of Molecular Genetics, Graduate School of Medical Science, Kanazawa University, Takara-machi, Kanazawa 920-8640, Japan
[6]Central Institute for Experimental Animals, Miyamae-ku, Kawasaki 216-0001, Japan

Stimulatory and inhibitory co-receptors play fundamental roles in the regulation of the immune system. We describe a new mouse model of spontaneous autoimmune disease. *Activation-induced cytidine deaminase–linked autoimmunity* (*aida*) mice harbor a loss-of-function mutation in the gene encoding lymphocyte activation gene 3 (LAG-3), an inhibitory co-receptor. Although LAG-3 deficiency alone did not induce autoimmunity in nonautoimmune-prone mouse strains, it induced lethal myocarditis in BALB/c mice deficient for the gene encoding the inhibitory co-receptor programmed cell death 1 (PD-1). In addition, LAG-3 deficiency alone accelerated type 1 diabetes mellitus in nonobese diabetic mice. These results demonstrate that LAG-3 acts synergistically with PD-1 and/or other immunoregulatory genes to prevent autoimmunity in mice.

CORRESPONDENCE
Taku Okazaki:
tokazaki@
genome.tokushima-u.ac.jp.

Abbreviations used: AID, activation-induced cytidine deaminase; *aida*, *AID-linked autoimmunity*; autoAb, autoantibody; CSR, class switch recombination; CTLA-4, cytotoxic T lymphocyte antigen 4; DCM, dilated cardiomyopathy; ILF, isolated lymphoid follicle; LAG-3, lymphocyte activation gene 3; NOD, nonobese diabetic; PD-1, programmed cell death 1; SHM, somatic hypermutation; SNP, single nucleotide polymorphism; SPF, specific pathogen free; T1DM, type 1 diabetes mellitus.

Most autoimmune diseases in human are polygenic, and multiple genetic alterations are involved in the initiation and progression of these diseases. Spontaneous animal models of autoimmune diseases are useful for the elucidation of genetic basis of autoimmune diseases because they have all genetic alterations required for the overt autoimmune diseases. To date, various kinds of animals that spontaneously develop autoimmune diseases have been selected, fixed, and used. Although most of them are regulated by many genetic alterations, as in human polygenic autoimmune diseases, there are a few models that are regulated by a single genetic alteration. Each genetic alteration in the latter type of model has a stronger influence on immune system than those in the former type of models, making it relatively easy to identify the causal mutation and to elucidate its function in immunological tolerance. For example, the forkhead box P3 gene (*Foxp3*) has been identified as a causal gene of the *scurfy* mouse (Brunkow et al., 2001), which led to the deeper understanding of not only regulatory T cells (T reg cells) but also follicular helper T cells (Fontenot et al., 2003; Hori et al., 2003; Khattri et al., 2003; Tsuji et al., 2009). However, the number of such models is quite limited.

Programmed cell death 1 (PD-1; mouse gene, *Pdcd1*), an immunoreceptor belonging to the CD28/cytotoxic T lymphocyte antigen 4 (CTLA-4; mouse gene, *Ctla4*) family, provides negative costimulation to antigen stimulation (Okazaki and Honjo, 2006; Keir et al., 2008). PD-1 knockout ($Pdcd1^{-/-}$) mice develop lupus-like glomerulonephritis and arthritis on the C57BL/6 background, autoimmune dilated cardiomyopathy (DCM) and gastritis on the BALB/c background, acute type 1 diabetes mellitus (T1DM) on the nonobese diabetic (NOD)

J. Wang's present address is Institute for Neuroscience, The Fourth Military Medical University, Xi'an 710032, China.
T. Yoshida and Y. Kato's present address is Tsukuba Research Laboratories, Eisai Co., Ltd., Tsukuba 300-2635, Japan.

The Rockefeller University Press $30.00
J. Exp. Med. Vol. 208 No. 2 395-407
www.jem.org/cgi/doi/10.1084/jem.20100466

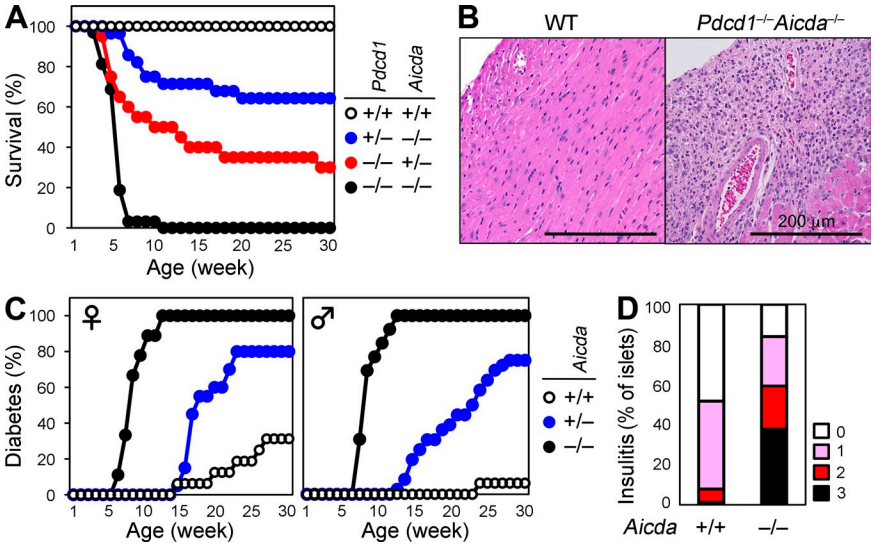

Figure 1. Spontaneous development of autoimmune diseases in AID-deficient mice. (A) Survival curves of BALB/c-*Pdcd1*$^{-/-}$*Aicda*$^{-/-}$ (n = 32), BALB/c-*Pdcd1*$^{-/-}$*Aicda*$^{+/-}$ (n = 20), BALB/c-*Pdcd1*$^{+/-}$*Aicda*$^{-/-}$ (n = 28), and BALB/c wild-type (n = 13) mice. (B) Representative histology of the heart from BALB/c wild-type and BALB/c-*Pdcd1*$^{-/-}$*Aicda*$^{-/-}$ mice. (C) Incidence of type 1 diabetes in NOD-*Aicda*$^{-/-}$, NOD-*Aicda*$^{+/-}$, and NOD wild-type female (left, n = 9, 20, and 16, respectively) and male (right, n = 13, 36, and 16, respectively) mice. (D) The percentage of islets with each grade of insulitis (0, 1, 2, and 3) in female NOD wild-type (+/+) and NOD-*Aicda*$^{-/-}$ (−/−) mice at 7 wk of age. More than 200 islets from five NOD wild-type and six NOD-*Aicda*$^{-/-}$ mice were analyzed.

background, and lethal myocarditis on the MRL background (Okazaki and Honjo, 2006; Wang et al., 2010), suggesting that PD-1 deficiency acts synergistically with other genetic alterations inherent to each strain to induce strain-specific autoimmune diseases.

Because autoimmune diseases in *Pdcd1*$^{-/-}$ mice frequently accompany the production of tissue-specific autoantibodies (autoAbs; Okazaki et al., 2003, 2005), they may provide especially useful insights on the regulation of autoreactive B cells. One of the unique features of B cells is the introduction of genetic modifications into immunoglobulin genes after maturation. The affinity of Ab to its cognate antigen can be improved by random somatic hypermutation (SHM) on immunoglobulin heavy and light chain genes and subsequent selection of B cell clones with increased affinity for the antigen. In addition, the isotype of Abs can be changed by class switch recombination (CSR) of immunoglobulin heavy chain constant region gene, which endows Abs with diverse effector functions (Honjo et al., 2002). Both of these genetic modifications are introduced by activation-induced cytidine deaminase (AID; mouse gene, *Aicda*), and *Aicda*$^{-/-}$ mice are defective in both SHM and CSR (Muramatsu et al., 1999, 2000). SHM and CSR are expected to play essential roles in the development of autoimmunity because isotype-switched and somatically mutated autoAbs are hallmarks of antigen-specific immune responses and they are frequently found in human patients and model animals of systemic and organ-specific autoimmune diseases (Shlomchik et al., 1990; van Es et al., 1991; Stott et al., 1998). However, the roles of SHM and CSR in autoimmune diseases are still controversial (Jiang et al., 2007; Chen et al., 2010).

In the present study, we crossed BALB/c-*Pdcd1*$^{-/-}$ with BALB/c-*Aicda*$^{-/-}$ mice to analyze the roles of SHM and CSR in the development of gastritis and DCM. Unexpectedly, all of the BALB/c-*Pdcd1*$^{-/-}$*Aicda*$^{-/-}$ mice died of severe myocarditis before 10 wk of age. However, subsequent analyses revealed this effect was not the result of AID deficiency but of a spontaneous loss-of-function mutation, which we named *AID-linked autoimmunity* (*aida*), in a neighboring gene, lymphocyte activation gene 3 (LAG-3; mouse gene, *Lag3*). Although LAG-3 deficiency alone did not induce autoimmunity in nonautoimmune-prone strains, it induced lethal myocarditis in the absence of PD-1 on the BALB/c background. In addition, LAG-3 deficiency alone exaggerated the onset and the penetrance of T1DM in NOD mice. These results indicate that LAG-3 is a critical regulator of autoimmunity and that it acts synergistically with PD-1 and/or other immune regulators to prevent autoimmunity in mice.

RESULTS

AID deficiency exaggerated autoimmune phenotypes of NOD mice and *Pdcd1*$^{-/-}$ mice

To analyze the roles of SHM and CSR of autoAb in the development of gastritis and DCM, we crossed BALB/c-*Pdcd1*$^{-/-}$ with BALB/c-*Aicda*$^{-/-}$ mice, which are defective in both the SHM and CSR (Muramatsu et al., 2000; Fagarasan et al., 2002). Unexpectedly, all of the BALB/c-*Pdcd1*$^{-/-}$*Aicda*$^{-/-}$ mice died before 10 wk of age (Fig. 1 A). Autopsy examination revealed that all of the BALB/c-*Pdcd1*$^{-/-}$*Aicda*$^{-/-}$ mice exhibited dilatation of the heart, with occasional thrombus formation in the atrium, pleural effusion, ascites, and congested liver, suggesting congestive heart failure as the cause of premature death. Histological examination revealed massive lymphocytic infiltration into the atrium and ventricle of the heart (Fig. 1 B). Lymphocyte infiltration was also occasionally found in the stomach, salivary gland, pancreas, lung, and liver, with little to no tissue destruction (Fig. S1). Intriguingly, ∼60% of BALB/c-*Pdcd1*$^{-/-}$*Aicda*$^{+/-}$ mice died of myocarditis, suggesting that AID protects mice from autoimmunity in a dose-dependent manner. To analyze the PD-1–independent effect of the AID deficiency, we backcrossed BALB/c-*Aicda*$^{-/-}$ mice on the NOD background. Both female and male NOD-*Aicda*$^{-/-}$ mice developed T1DM much faster than NOD wild-type mice, and all of the NOD-*Aicda*$^{-/-}$ mice developed T1DM before 13 wk of age (Fig. 1 C).

Histological examination revealed more severe insulitis in the NOD-*Aicda*$^{-/-}$ than in the NOD wild-type mice, confirming that the exacerbation of T1DM was a result of the augmented autoimmune response against the β cells in islets (Fig. 1 D). Again, we observed a dose effect of AID on the regulation of T1DM.

AID deficiency exaggerated autoimmunity in the absence of B cells

We previously reported that *Aicda*$^{-/-}$ mice show hyperplasia of the isolated lymphoid follicles (ILFs), with a 100-fold expansion of anaerobic flora (Fagarasan et al., 2002). Therefore, we examined the effect of flora on the acceleration of autoimmunity by generating germ-free NOD-*Aicda*$^{-/-}$ mice. Against our expectations, the germ-free NOD-*Aicda*$^{-/-}$ mice developed T1DM at a comparable frequency to that of littermate NOD-*Aicda*$^{-/-}$ mice that had been moved from the germ-free to a specific pathogen-free (SPF) environment at 5 wk of age (Fig. 2 A). Therefore, the exaggeration of T1DM by the AID deficiency was not a result of the expansion of commensal microorganisms. Next, we examined the involvement of B cells by crossing B cell–deficient NOD-μMT mice with NOD-*Aicda*$^{-/-}$ mice. Surprisingly, the AID deficiency also accelerated the onset of T1DM in the absence of B cells, suggesting that the AID deficiency affects non–B cells to accelerate T1DM (Fig. 2 B). Because recent findings suggest that AID functions in nonlymphoid as well as lymphoid tissues (Okazaki et al., 2002; Endo et al., 2007; Matsumoto et al., 2007), we hypothesized that AID modifies the antigenicity of a certain β cell antigen by introducing somatic mutations. However, the adoptive transfer of BM cells from NOD wild-type mice induced T1DM with a similar time course in NOD-SCID and NOD-SCID-*Aicda*$^{-/-}$ mice, whereas the adoptive transfer of BM cells from NOD-*Aicda*$^{-/-}$ mice induced T1DM in NOD-SCID mice more quickly (Fig. 2 C). In addition, adoptive transfer experiments showed that the effector cells of myocarditis in the BALB/c-*Pdcd1*$^{-/-}$*Aicda*$^{-/-}$ mice were CD4^{+} T cells (Fig. 2 D). These results suggested that the AID deficiency affects T cells, rather than B cells, to accelerate autoimmunity.

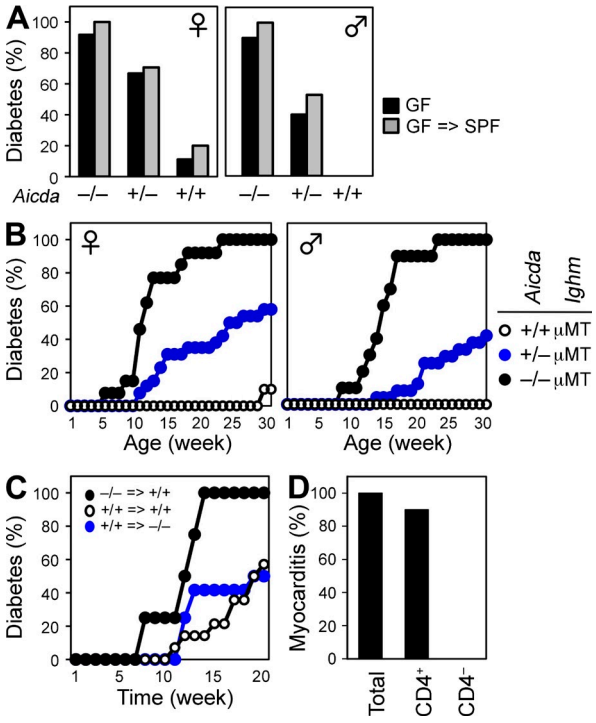

Figure 2. B cells are not required for the spontaneous development of autoimmune diseases in AID-deficient mice. (A) Incidence of type 1 diabetes by 18 wk in female (left) and male (right) NOD-*Aicda*$^{-/-}$ (−/−), NOD-*Aicda*$^{+/-}$ (+/−), and NOD wild-type (+/+) mice that were kept in germ-free conditions (GF; *n* = 13, 9, and 8 for female and *n* = 10, 5, and 12 for male mice, respectively) or moved to SPF conditions (GF => SPF) at 5 wk of age (*n* = 11, 17, and 5 for female and *n* = 5, 17, and 6 for male mice, respectively). (B) Incidence of type 1 diabetes in NOD-μMT-*Aicda*$^{-/-}$, NOD-μMT-*Aicda*$^{+/-}$, and NOD-μMT female (*n* = 13, 26, and 10, respectively) and male (*n* = 10, 24, and 17, respectively) mice. *Ighm*, immunoglobulin heavy constant mu gene. (C) Incidence of type 1 diabetes in NOD-SCID recipients of wild-type NOD BM (+/+ => +/+, *n* = 12) and NOD-SCID-*Aicda*$^{-/-}$ recipients of wild-type NOD BM (+/+ => −/−, *n* = 14), and NOD-SCID recipients of NOD-*Aicda*$^{-/-}$ BM (−/− => +/+, *n* = 4). (D) Incidence of myocarditis by 7 wk after the adoptive transfer of total (*n* = 4), CD4^{+} (*n* = 10), or CD4-depleted (*n* = 19) spleen cells from moribund BALB/c-*Pdcd1*$^{-/-}$*Aicda*$^{-/-}$ mice into BALB/c-*Rag2*$^{-/-}$ mice.

Isolation of autoimmune-resistant lines of *Aicda*$^{-/-}$ mice and establishment of *aida* mice

Among >50 BALB/c-*Pdcd1*$^{-/-}$*Aicda*$^{-/-}$ mice generated, one male mouse survived longer than 20 wk, suggesting that the acceleration of autoimmunity was not a result of the defect in AID function but of a mutation in another gene closely associated with *Aicda*. We named this mutation *aida* for AID-linked autoimmunity and tried to isolate myocarditis-resistant and -susceptible lines. Because this myocarditis-free male mouse was expected to be heterozygous for *aida*, we mated this mouse with female BALB/c-*Pdcd1*$^{-/-}$ mice to obtain male BALB/c-*Pdcd1*$^{-/-}$*Aicda*$^{+/-}$ mice, half of which were expected to carry a single *aida* locus. We further mated these male F1 progenies with female BALB/c wild-type mice to obtain female BALB/c-*Pdcd1*$^{+/-}$*Aicda*$^{+/-}$ mice and backcrossed each female F2 progeny to its F1 father. As expected, some mating pairs yielded only myocarditis-susceptible BALB/c-*Pdcd1*$^{-/-}$*Aicda*$^{-/-}$ mice and the others yielded only myocarditis-resistant BALB/c-*Pdcd1*$^{-/-}$*Aicda*$^{-/-}$ mice. We used BALB/c-*Pdcd1*$^{+/-}$*Aicda*$^{-/-}$ mice from each type of litters for the subsequent mating and established myocarditis-resistant (lines K and Y) and -susceptible (lines D and X) lines. We could also isolate T1DM-resistant and -susceptible lines of NOD-μMT-*Aicda*$^{-/-}$ mice.

Identification of LAG-3 as a causal gene of *aida* mice

Because the *Aicda*$^{-/-}$ mice were generated by disrupting *Aicda* in TT2 ES cells, which were established from (CBA × C57BL/6)$_{F1}$ embryo (Yagi et al., 1993), the origin of the chromosome surrounding *Aicda* was C57BL/6, CBA, or

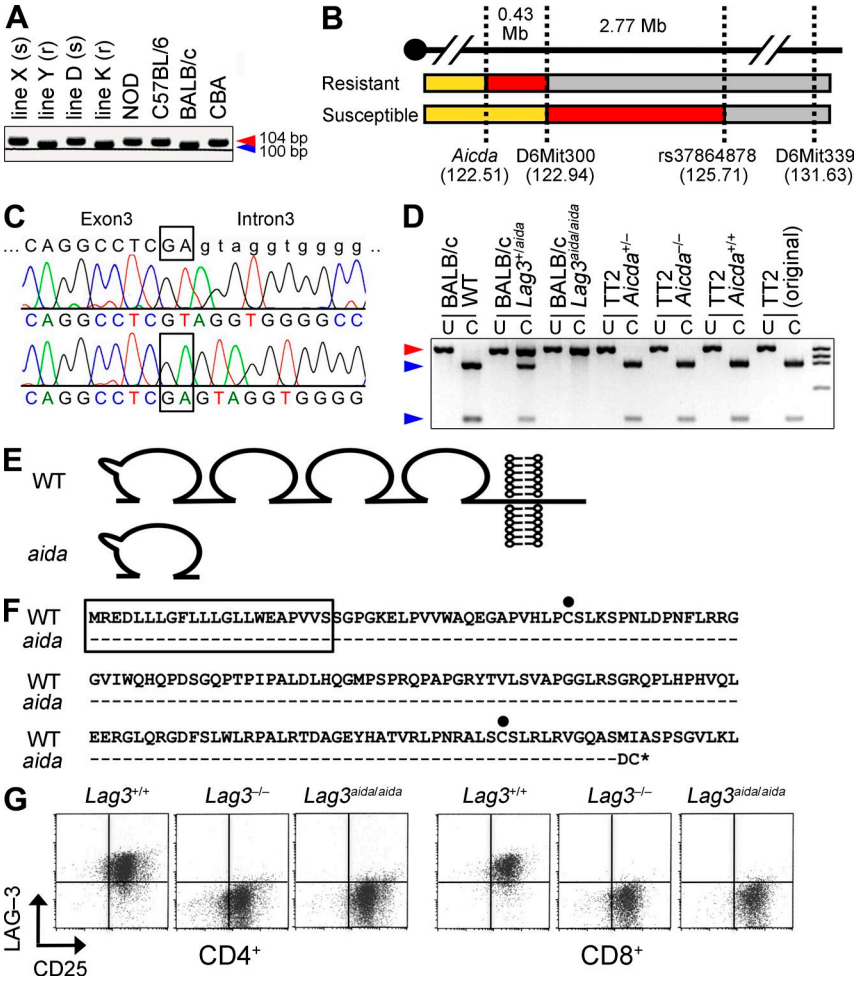

Figure 3. Identification of a 2-bp deletion in the LAG-3 gene. (A) Presence of CBA- or BALB/c-derived alleles at D6Mit300 in myocarditis-susceptible (X and D) and -resistant (Y and K) mouse lines was analyzed by simple sequence length polymorphism (SSLP). Representative data of more than three independent experiments are shown. (B) Origins of the chromosomal regions for the myocarditis-resistant (top) and -susceptible (bottom) BALB/c-*Pdcd1*$^{-/-}$*Aicda*$^{-/-}$ lines. CBA, yellow; undetermined, red; BALB/c, gray. The causal gene was mapped between *Aicda* and rs37864878. (C) Sequencing of the mouse LAG-3 gene of disease-susceptible (top) and -resistant (bottom) mouse lines, with a reference sequence (http://ncbi.nlm.nih.gov). Bases deleted in susceptible strain are boxed. Representative data of more than three independent experiments are shown. (D) Restriction fragment length polymorphism (RFLP) analysis of the LAG-3 gene in BALB/c wild-type mice, BALB/c-*Lag3*$^{+/aida}$ mice, BALB/c-*Lag3*$^{aida/aida}$ mice, TT2-*Aicda*$^{+/-}$ ES cells, TT2-*Aicda*$^{-/-}$ ES cells, TT2 ES cells (maintained in our laboratory), and TT2 ES cells (purchased from a distributor) genomes. U, uncut; C, cut. Blue and red triangles indicate the bands from cut wild-type and mutant *aida* alleles, respectively. Representative data of more than three independent experiments are shown. (E) Schematic representations of wild-type and *aida* mutant LAG-3 proteins are shown. LAG-3 is composed of the extracellular region with four immunoglobulin-like domains, transmembrane region, and cytoplasmic region. (F) Predicted amino acid sequence of the *aida* mutant LAG-3 is shown in relation to the first immunoglobulin domain of wild-type LAG-3. A predicted signal sequence is boxed. Dashes represent no difference between the *aida* and wild-type LAG-3. Asterisk represents a premature stop codon. Cysteine residues involved in the immunoglobulin fold are marked by black dots. (G) Splenocytes from indicated mice were stimulated with 3 µg/ml of plate-bound anti-CD3 Abs for 24 h, and the expression of LAG-3 was analyzed by flow cytometry. Left dot plots are gated on CD4$^+$ cells and right dot plots are gated on CD8$^+$ cells. Representative flow cytometric profiles of three independent experiments are shown.

BALB/c in the BALB/c-*Aicda*$^{-/-}$ mice and C57BL/6, CBA, BALB/c, or NOD in the NOD-*Aicda*$^{-/-}$ mice. Because microsatellite marker analyses revealed that the targeting construct of *Aicda* was integrated into CBA-derived chromosome (unpublished data) and the disease-resistant lines were isolated in the course of backcrossing on BALB/c and NOD strains, the *aida* mutation was likely an inherent polymorphism of the CBA strain. Therefore, we sought to determine the origin of the chromosome in disease-susceptible and -resistant lines more in detail using microsatellite and single nucleotide polymorphism (SNP) markers.

Among >50 markers examined, D6Mit300 distinguished the disease-resistant and -susceptible lines. As expected, disease susceptibility was associated with the CBA allele at D6Mit300 (122,941,371 bp from the centromere; Fig. 3 A). Because both disease-susceptible and -resistant lines harbored the BALB/c-derived chromosome at rs37864878 (125,714,481 bp), the causal gene was expected to exist in the region between *Aicda* (122,514,197 bp) and rs37864878 (Fig. 3 B). Because there are nearly 100 genes in this region, we selected genes that are expected to engage in immune response and sequenced their exons (Table S1). We found a 2-bp deletion in the LAG-3 gene (124,854,379 bp) of the disease-susceptible line (Fig. 3 C; Triebel et al., 1990). Against our expectations, the deletion was not found in the genomes of the TT2 embryonic stem cells or the CBA wild-type mice (Fig. 3 D and not depicted). In addition, the deletion was not found in the genomes of C57BL/6-*Pdcd1*$^{-/-}$*Aicda*$^{-/-}$ mice that did not show any overt autoimmune phenotypes by 24 wk of age (unpublished data). Collectively, it is likely that this deletion was accidentally introduced into CBA-derived *Lag3* and passed on together with the knockout allele of *Aicda* in the course of backcrossing onto the BALB/c background. The 2-bp deletion was predicted to cause a frame shift and introduce a premature stop codon right after the first immunoglobulin fold of LAG-3 (Fig. 3, E and F).

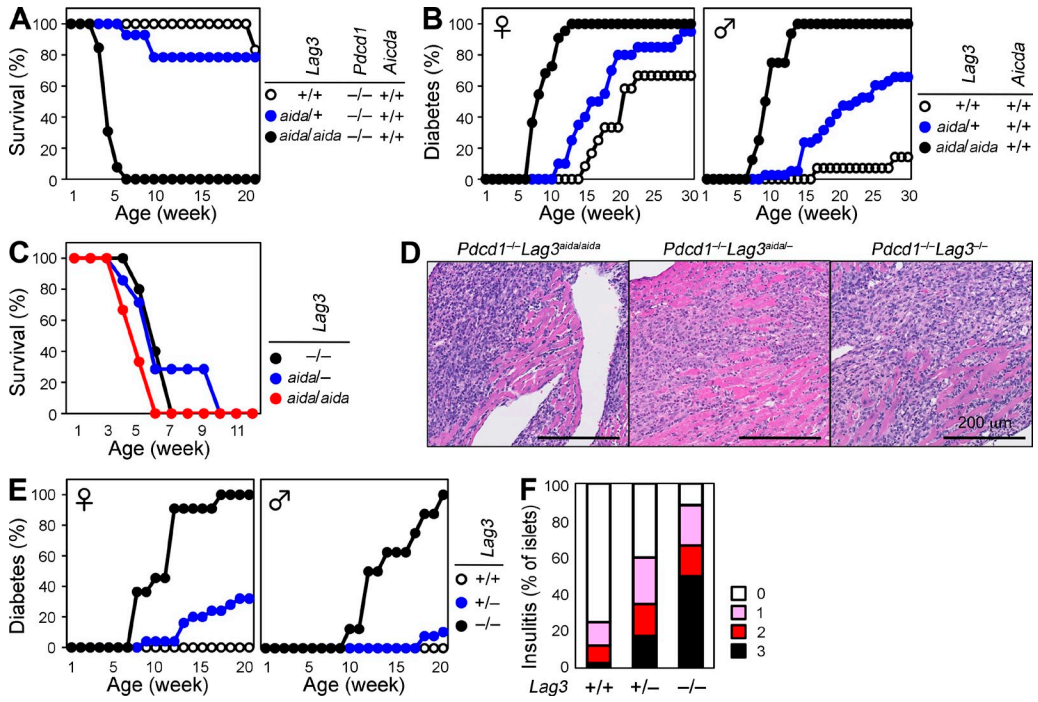

Figure 4. LAG-3 deficiency causes the autoimmunity in *aida* mice. (A) Survival curves of BALB/c-*Pdcd1*$^{-/-}$*Lag3*$^{aida/aida}$ (n = 13), BALB/c-*Pdcd1*$^{-/-}$*Lag3*$^{+/aida}$ (n = 14), and BALB/c-*Pdcd1*$^{-/-}$ (n = 6) mice. (B) Type 1 diabetes incidence in NOD-*Lag3*$^{aida/aida}$, NOD-*Lag3*$^{+/aida}$, and NOD wild-type female (n = 12, 20, and 22, respectively) and male (n = 14, 38, and 16, respectively) mice. (C) Survival curves of BALB/c-*Pdcd1*$^{-/-}$*Lag3*$^{-/-}$ (n = 5), BALB/c-*Pdcd1*$^{-/-}$*Lag3*$^{aida/-}$ (n = 7), and BALB/c-*Pdcd1*$^{-/-}$*Lag3*$^{aida/aida}$ (n = 3) mice. (D) Representative histology of the heart from BALB/c-*Pdcd1*$^{-/-}$*Lag3*$^{aida/aida}$, BALB/c-*Pdcd1*$^{-/-}$*Lag3*$^{aida/-}$, and BALB/c-*Pdcd1*$^{-/-}$*Lag3*$^{-/-}$ mice. (E) Type 1 diabetes incidence in NOD-*Lag3*$^{-/-}$, NOD-*Lag3*$^{+/-}$, and NOD wild-type female (n = 15, 25, and 11, respectively) and male (n = 17, 38, and 18, respectively) mice. (F) Percentage of islets with each grade of insulitis (0, 1, 2, and 3) in 8-wk-old female NOD mice with the indicated genotype. More than 100 islets from five *Lag3*$^{-/-}$, three *Lag3*$^{+/-}$, and four wild-type mice were analyzed.

Consistent with this prediction, LAG-3 protein could not be detected on the surface of CD4$^+$ or CD8$^+$ T cells from *aida* mice (Fig. 3 G). LAG-3, a type I transmembrane protein that shares various features with CD4, is expressed on activated T cells, NK cells, and plasmacytoid DCs (Triebel et al., 1990; Miyazaki et al., 1996; Workman et al., 2002b). Although the precise signaling mechanism is unclear, several groups have shown that LAG-3 negatively regulates T cell activation and proliferation (Hannier et al., 1998; Workman and Vignali, 2003; Workman et al., 2004; Grosso et al., 2007). Therefore, it seemed very likely that this mutation was the causal mutation of the *aida* phenotype, and we therefore called this mutant allele *Lag3*^{aida}.

Aida mutation exaggerated autoimmunity irrespectively of AID

We then segregated the *Lag3*$^{aida/aida}$ from *Aicda*$^{-/-}$ to generate BALB/c-*Pdcd1*$^{-/-}$*Lag3*$^{aida/aida}$ and NOD-*Lag3*$^{aida/aida}$ mice. The BALB/c-*Pdcd1*$^{-/-}$*Lag3*$^{aida/aida}$ mice died of myocarditis in a similar time course as the BALB/c-*Pdcd1*$^{-/-}$*Aicda*$^{-/-}$*Lag3*$^{aida/aida}$ mice (compare Fig. 4 A with Fig. 1 A), and NOD-*Lag3*$^{aida/aida}$ mice developed T1DM as quickly as NOD-*Aicda*$^{-/-}$*Lag3*$^{aida/aida}$ mice (compare Fig. 4 B with Fig. 1 C), indicating that the AID deficiency was not required for the acceleration of autoimmunity. *Lag3*$^{-/-}$ mice were originally reported by Miyazaki et al. (1996) to be defective in the cytotoxicity of NK cells against MHC class I–negative targets but normal in diverse aspects of T cell function. Because no spontaneous manifestation of autoimmunity has been reported for *Lag3*$^{-/-}$ mice, we backcrossed the C57BL/6-*Lag3*$^{-/-}$ mice on the BALB/c and NOD background. As expected, all of the BALB/c-*Pdcd1*$^{-/-}$*Lag3*$^{-/-}$ mice died of myocarditis as quickly as the BALB/c-*Pdcd1*$^{-/-}$*Lag3*$^{aida/aida}$ mice (Fig. 4, C and D), and the NOD-*Lag3*$^{-/-}$ mice developed T1DM much earlier (Fig. 4 E) and showed more severe insulitis (Fig. 4 F) than the NOD wild-type mice. These results confirmed that the loss-of-function mutation in *Lag3* was responsible for the acceleration of autoimmunity that was originally linked to the *Aicda* knockout allele.

Hyperplasia of ILFs was dependent on AID deficiency but not *aida* mutation

The identification of the *aida* mutation on *Lag3* may bring some previous studies using BALB-*Aicda*$^{-/-}$ mice into question. *Aicda*$^{-/-}$ mice have been shown to develop hyperplasia of the ILFs with a 100-fold expansion of the anaerobic flora (Fagarasan et al., 2002). Examination of the small intestine revealed a large number of enlarged ILFs in the intestines of the BALB/c-*Aicda*$^{-/-}$ but not the BALB/c-*Lag3*$^{aida/aida}$ mice, indicating that the hyperplasia of the ILFs was actually a result of AID deficiency and not of LAG-3 deficiency (Fig. 5).

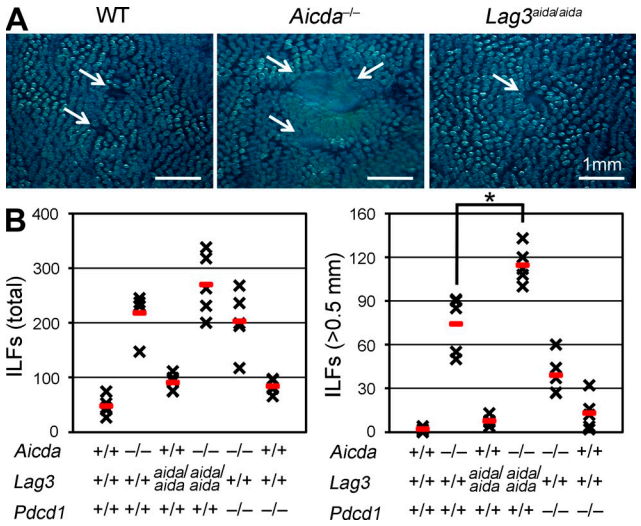

Figure 5. Hyperplasia of ILFs is dependent on AID deficiency but not on LAG-3 deficiency. (A) Representative pictures of the ILFs in BALB/c wild-type, BALB/c-*Aicda*$^{-/-}$, and BALB/c-*Lag3*$^{aida/aida}$ mice. Arrows indicate ILFs. (B) The number of total (left) and large (right, >0.5 mm) ILFs was evaluated in mice with the indicated genotype at ∼21–23 wk of age (n = 6 each). Each black symbol represents an individual mouse and the red bar represents the mean value for each group. *, $P < 0.05$.

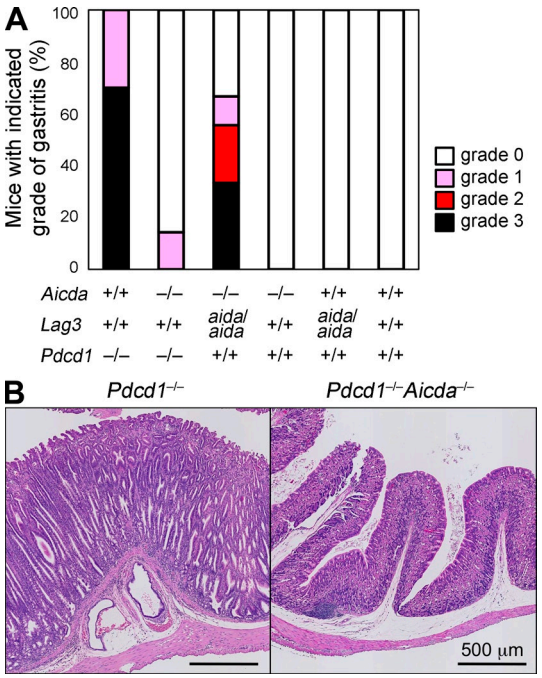

Figure 6. Gastritis in BALB/c-*Pdcd1*$^{-/-}$ mice requires autoAbs that have undergone SHM and/or CSR. (A) Incidence of gastritis of indicated grade (0, 1, 2, and 3) at 21–23 wk of age in BALB/c-*Pdcd1*$^{-/-}$ (n = 10), BALB/c-*Aicda*$^{-/-}$*Pdcd1*$^{-/-}$ (n = 7), BALB/c-*Aicda*$^{-/-}$*Lag3*$^{aida/aida}$ (n = 9), BALB/c-*Aicda*$^{-/-}$ (n = 6), BALB/c-*Lag3*$^{aida/aida}$ (n = 6), and BALB/c wild-type (n = 5) mice. (B) Representative histology of the stomach of BALB/c-*Pdcd1*$^{-/-}$ and BALB/c-*Pdcd1*$^{-/-}$*Aicda*$^{-/-}$ mice.

However, the LAG-3 deficiency seemed to exaggerate the size of the ILFs formed in the intestines of BALB/c-*Aicda*$^{-/-}$ mice because the number of large (>0.5 mm) ILFs, but not total ILFs, was significantly increased in the BALB/c-*Aicda*$^{-/-}$*Lag3*$^{aida/aida}$ mice compared with the BALB/c-*Aicda*$^{-/-}$ mice (Fig. 5 B; $P < 0.01$ and $P > 0.1$, respectively). Spontaneous germinal center formation in the BALB/c-*Aicda*$^{-/-}$ mice was also dependent on the AID deficiency and not the LAG-3 deficiency because the number of PNA^{+} B cells in the spleen and Peyer's patches are increased in BALB/c-*Aicda*$^{-/-}$ but not in the BALB/c-*Lag3*$^{aida/aida}$ mice (Fig. S2; Muramatsu et al., 2000; Fagarasan et al., 2002).

Gastritis and DCM of BALB/c-*Pdcd1*$^{-/-}$ mice required SHM and CSR

At this point, we were able to examine the original question of whether AID deficiency affects the autoimmune phenotypes of BALB/c-*Pdcd1*$^{-/-}$ mice. Gastritis was almost completely abolished by the AID deficiency (Fig. 6), indicating that gastritis in BALB/c-*Pdcd1*$^{-/-}$ mice requires autoAbs and/or autoreactive B cells that have undergone SHM and/or CSR. Interestingly, ∼60% of the BALB/c-*Aicda*$^{-/-}$*Lag3*$^{aida/aida}$ mice, but none of the BALB/c-*Aicda*$^{-/-}$ or BALB/c-*Lag3*$^{aida/aida}$ mice, developed substantial gastritis. The incidence of DCM in BALB/c-*Pdcd1*$^{-/-}$ mice varies from 0 to 60% among colonies (Okazaki and Honjo, 2006). The incidence of DCM was 20% in the current colony of BALB/c-*Pdcd1*$^{-/-}$ mice (N14) and 0% in the BALB/c-*Pdcd1*$^{-/-}$*Aicda*$^{-/-}$ mice (Fig. S3). Therefore, DCM in BALB/c-*Pdcd1*$^{-/-}$ mice also requires autoAbs and/or autoreactive B cells that have undergone SHM and/or CSR.

Augmented Th1 response in BALB/c-*Pdcd1*$^{-/-}$*Lag3*$^{aida/aida}$ mice

To analyze the mechanisms of how compound deficiency of PD-1 and LAG-3 induces myocarditis, we first analyzed the activation status of splenocytes. LAG-3 deficiency slightly increased the number of lymphocytes on the BALB/c and NOD backgrounds in accordance with a previous study on C57BL/6-*Lag3*$^{-/-}$ mice (Workman and Vignali, 2005), whereas the number of lymphocytes was not increased in BALB/c-*Pdcd1*$^{-/-}$*Lag3*$^{aida/aida}$ mice (Fig. 7, A and B). The frequency of activated T cells (CD44^{+}CD62L^{-}) in spleen was significantly increased in BALB/c-*Pdcd1*$^{-/-}$*Lag3*$^{aida/aida}$ mice but not in NOD-*Lag3*$^{aida/aida}$ mice (Fig. 7, C and D). Next, we analyzed heart infiltrates and found that CD4^{+} and CD8^{+} T cells constituted 18.7 and 30.0% of heart infiltrates, respectively (Fig. 7 E), and they were highly activated judging from the expression profiles of CD62L and CD44 (Fig. 7 C).

Upon activation with PMA and ionomycin for 5 h, >40% of heart infiltrating CD4^{+} T cells and >80% of heart infiltrating CD8^{+} T cells produced IFN-γ, whereas IL-4– and IL-17–producing cells were much less (IL-4, 1.3 ± 0.12% and 0.03 ± 0.00%; IL-17, 0.48 ± 0.13% and 0.08 ± 0.02%, respectively for CD4^{+} and CD8^{+} T cells), suggesting that heart-infiltrating T cells were biased to Th1 (Fig. 7, F and G). Consistently, the inflamed heart contained a larger amount of mRNA of IFN-γ, but not IL-1,

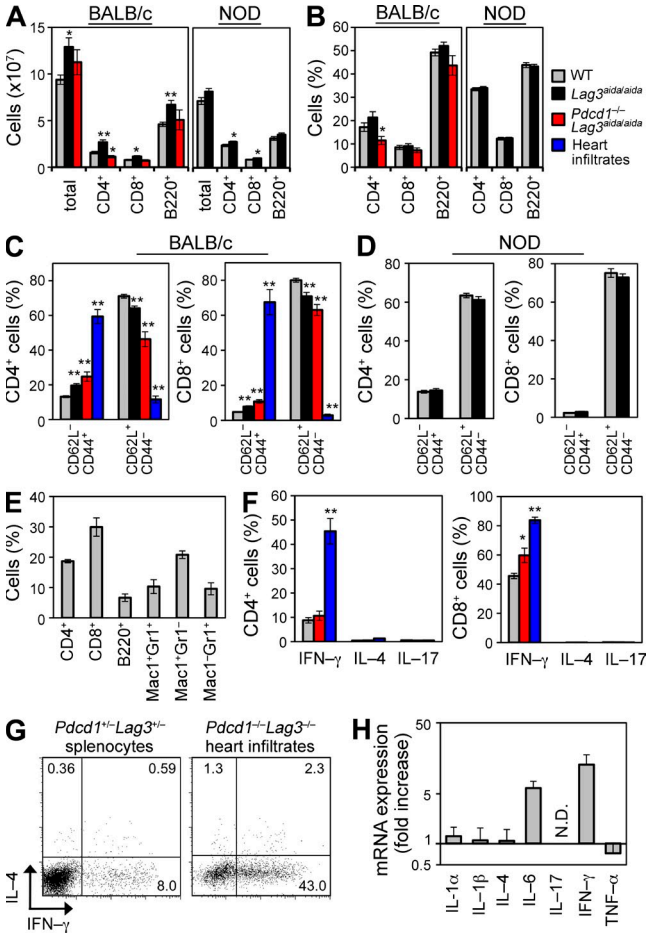

Figure 7. Augmented Th1-response in BALB/c-*Pdcd1*$^{-/-}$*Lag3*$^{aida/aida}$ mice. (A and B) The absolute number (A) and frequency (B) of each cell fraction in spleen of mice of indicated genotypes at 3–6 wk of age. (C and D) Frequencies of activated ($CD62L^{-}CD44^{+}$) and naive ($CD62L^{+}CD44^{-}$) $CD4^{+}$ and $CD8^{+}$ T cells in spleen of mice of indicated genotypes. (E) Frequencies of indicated cell fraction in $CD45^{+}$ heart infiltrates from BALB/c-*Pdcd1*$^{-/-}$*Lag3*$^{-/-}$ mice are shown. (F and G) Frequencies of $CD4^{+}$ and $CD8^{+}$ T cells that produced IFN-γ, IL-4, and IL-17 upon ex vivo stimulation. Splenocytes of BALB/c-*Pdcd1*$^{+/-}$*Lag3*$^{+/-}$ and BALB/c-*Pdcd1*$^{-/-}$*Lag3*$^{-/-}$ mice and heart infiltrates of BALB/c-*Pdcd1*$^{-/-}$*Lag3*$^{-/-}$ mice were analyzed. Representative flow cytometric profiles are shown in G. (H) Quantities of mRNA encoding indicated genes in inflamed hearts of BALB/c-*Pdcd1*$^{-/-}$*Lag3*$^{aida/aida}$ mice relative to that in spleens of BALB/c wild-type mice. Data are mean ± SEM (A–F) or mean + SEM (H). N.D., not detected. **, $P < 0.01$; *, $P < 0.05$. At least three mice of each genotype were analyzed in each experiment. Data of three BALB/c-*Pdcd1*$^{-/-}$*Lag3*$^{aida/aida}$ and seven BALB/c-*Pdcd1*$^{-/-}$*Lag3*$^{-/-}$ mice are combined in A–C.

IL-4, IL-17, and TNF, compared with the spleen of control mice (Fig. 7 H).

T reg cells were normal in BALB/c-*Pdcd1*$^{-/-}$*Lag3*$^{aida/aida}$ mice

Because LAG-3 has been shown to play a role in T reg cell function and myocarditis is one of the frequent phenotypes of T reg cell failure, we analyzed the function of T reg cells in BALB/c-*Pdcd1*$^{-/-}$*Lag3*$^{aida/aida}$ mice (Tivol et al., 1995; Waterhouse et al., 1995; Huang et al., 2004). The frequency of $CD25^{+}FoxP3^{+}$ T reg cells was rather increased in BALB/c-*Pdcd1*$^{-/-}$*Lag3*$^{aida/aida}$ mice but unchanged in NOD-*Lag3*$^{aida/aida}$ mice compared with their controls (Fig. 8, A and B). The suppressive function of T reg cells from BALB/c-*Pdcd1*$^{-/-}$*Lag3*$^{aida/aida}$ mice was comparable to that of control T reg cells in an in vitro assay. In addition, responder cells from BALB/c-*Pdcd1*$^{-/-}$*Lag3*$^{aida/aida}$ and BALB/c wild-type mice were suppressed to a similar extent by T reg cells from either BALB/c wild-type or BALB/c-*Pdcd1*$^{-/-}$*Lag3*$^{aida/aida}$ mice (Fig. 8, C–F).

We then generated BM chimera of BALB/c-*Pdcd1*$^{-/-}$*Lag3*$^{aida/aida}$ and BALB/c wild-type mice, in which, theoretically, all kinds of regulatory cells originated from wild-type mice could be supplemented from the initiation step of autoimmunity. Adoptive transfer of BM cells from BALB/c-*Pdcd1*$^{-/-}$*Lag3*$^{aida/aida}$ mice into immunodeficient mice induced myocarditis within 6 wk. Strikingly, cotransfer of BM cells from BALB/c wild-type or BALB/c-*Lag3*$^{aida/aida}$ mice failed to suppress myocarditis, suggesting that myocarditis in BALB/c-*Pdcd1*$^{-/-}$*Lag3*$^{aida/aida}$ mice was not the result of a failure in cells with regulatory function (Fig. 8, G and H).

LAG-3 and PD-1 act synergistically to suppress T cell activation

To elucidate the co-operative roles of LAG-3 and PD-1, we examined the expression of these inhibitory receptors on T cells. Although these receptors were rarely expressed on freshly isolated T cells, they were rapidly induced on both $CD4^{+}$ and $CD8^{+}$ T cells upon stimulation with anti-CD3 Ab. Co-stimulation through CD28 up-regulated the expression level of these molecules. Interestingly, LAG-3 induction required a weaker stimulation than PD-1 induction (Fig. 9, A and B).

Next, we examined the inhibitory function of these receptors using DO11.10 cells that recognize OVA peptide on MHC class II molecule but lack CD4 expression. Because DO11.10 cells constitutively expressed PD-1 but not LAG-3, we introduced mouse LAG-3 cDNA into DO11.10 cells by retroviral infection. We also introduced mouse PD-L1 cDNA into IIA1.6 cells, an Fc receptor–negative B cell line, and used them for antigen presentation. LAG-3 and PD-1 suppressed IL-2 production by DO11.10 cells upon antigen stimulation. In addition, co-engagement of LAG-3 and PD-1 further suppressed IL-2 production, suggesting that LAG-3 and PD-1 act synergistically to suppress antigen stimulation of $CD4^{+}$ T cells (Fig. 9 C). We also examined the inhibitory function of LAG-3 using a CD4-positive cell line, 2B4.11 cells, that recognize a cytochrome *c* peptide. LAG-3 clearly inhibited IL-2 production by 2B4.11 cells upon antigen stimulation (Fig. S4).

We then examined the function of PD-1 and LAG-3 using primary mouse T cells. Naive $CD4^{+}$ T cells from DO11.10 transgenic mice that lack PD-1, LAG-3, or both were stimulated with antigen-loaded IIA1.6 cells expressing PD-L1. PD-1 and LAG-3 significantly inhibited proliferative response of primary DO11.10 T cells upon antigen stimulation. We could also observe an additive effect of PD-1 and LAG-3 (Fig. 9, D and E).

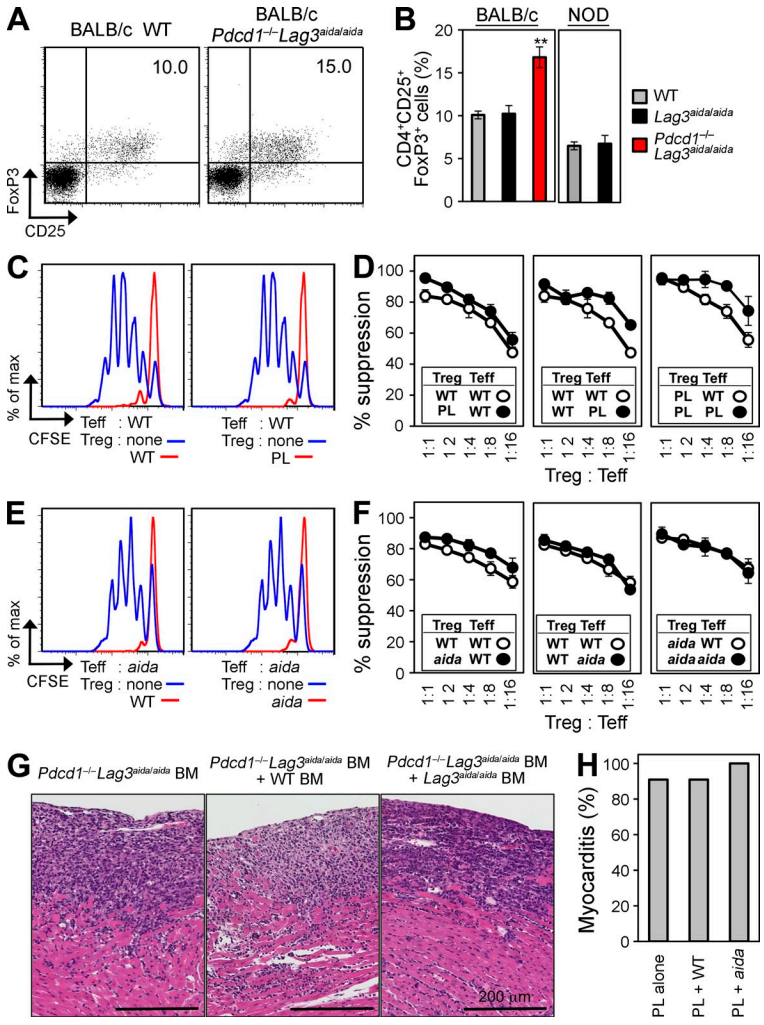

Figure 8. T reg cells were normal in BALB/c-*Pdcd1*$^{-/-}$*Lag3*$^{aida/aida}$ mice. (A and B) Frequencies of CD25$^+$FoxP3$^+$ T cells among CD4$^+$ T cells in spleen of wild-type (n = 9 and 9 for BALB/c and NOD, respectively), *Lag3*$^{aida/aida}$ (n = 6 and 9 for BALB/c and NOD, respectively), and *Pdcd1*$^{-/-}$*Lag3*$^{-/-}$ (n = 10; seven BALB/c-*Pdcd1*$^{-/-}$*Lag3*$^{-/-}$ and three BALB/c-*Pdcd1*$^{-/-}$*Lag3*$^{aida/aida}$) mice. Representative flow cytometric profiles are shown in A. Data are mean ± SEM. **, P < 0.01. (C–F) In vitro suppressor assay using CD4$^+$CD25$^+$ T reg cells and CFSE-labeled CD4$^+$CD25$^-$ effector cells (Teffs) from mice with the indicated genotype. The numbers on the x-axis indicate the ratio of CD4$^+$CD25$^+$ T reg cells to CD4$^+$CD25$^-$ effector T cells. WT, BALB/c wild-type; PL, BALB/c-*Pdcd1*$^{-/-}$*Lag3*$^{aida/aida}$; *aida*, BALB/c-*Lag3*$^{aida/aida}$ mice. Representative flow cytometric profiles of CFSE dilution (C and E). Mean ± SD of triplicate cultures are shown (D and F). Representative data of four (C and D) and two (E and F) independent experiments are shown. (G and H) Myocarditis in BALB/c-*Rag2*$^{-/-}$ mice reconstituted with BM from BALB/c-*Pdcd1*$^{-/-}$*Lag3*$^{aida/aida}$ and/or BALB/c wild-type mice. The frequency of myocarditis (H) and representative histology (G) are shown for BALB/c-*Rag2*$^{-/-}$ mice reconstituted with BM cells from BALB/c-*Pdcd1*$^{-/-}$*Lag3*$^{aida/aida}$ mice (n = 11), mixed BM cells from BALB/c-*Pdcd1*$^{-/-}$*Lag3*$^{aida/aida}$ and wild–type mice (n = 11), and mixed BM cells from BALB/c-*Pdcd1*$^{-/-}$*Lag3*$^{aida/aida}$ and BALB/c-*Lag3*$^{aida/aida}$ mice (n = 6).

DISCUSSION

In the current study, we have accidentally isolated a mouse line that spontaneously develops autoimmune diseases under the presence of other autoimmune susceptibility, named this line *aida* for AID-linked autoimmunity, and pursued its causal gene. After careful examination of neighboring genes of *Aicda*, we identified *Lag3* as a causal gene of *aida* mice. As summarized in Table S2, LAG-3 deficiency, but not AID deficiency, induced lethal myocarditis in the absence of PD-1 on the BALB/c background and it also exaggerated the onset and the penetrance of T1DM on the NOD background. LAG-3 is a type I transmembrane protein that shares various features with CD4. *Lag3*$^{-/-}$ mice were originally reported to be defective in the cytotoxicity of NK cells against MHC class I–negative targets but normal in diverse aspects of T cell function including positive and negative selection of T cells in thymus, numbers and distribution of peripheral CD4$^+$ and CD8$^+$ T cells, their activated and memory subpopulations and their responses to mitogens and antigen priming, B cell maturation and distribution, and Ab production after primary and secondary immunization by Miyazaki et al. (1996). Because the phenotype was much weaker than that of *Cd4*$^{-/-}$ mice, LAG-3 was not analyzed vigorously until recently.

Recently, LAG-3 has attracted increasing attention. LAG-3 was reported to negatively regulate the function of CD4$^+$ T cells, CD8$^+$ T cells, and plasmacytoid DCs (Grosso et al., 2007; Workman et al., 2009) and to regulate the homeostatic proliferation of CD8$^+$ T cells and the suppressive activity of T reg cells (Huang et al., 2004; Workman and Vignali, 2005). However, the effect of LAG-3 in these assays is relatively small, and the actual contribution of LAG-3 to the regulation of immune system has been unclear. In the current study, the LAG-3 deficiency was accidentally coupled with the PD-1 deficiency in vivo, which led us to discover that the inhibitory signal through LAG-3 is actually indispensable for robust immunological self-tolerance.

LAG-3 has been shown to play a role in T reg cell function, and myocarditis is one of the frequent phenotypes of T reg cell failure (Tivol et al., 1995; Waterhouse et al., 1995; Huang et al., 2004). In *Ctla4*$^{-/-}$ mice, spleens and lymph nodes are extremely enlarged (5–10-fold enlargement) and most of the peripheral T cells are activated and invade various organs, including the heart, resulting in the premature death around 3 wk of age (Tivol et al., 1995; Waterhouse et al., 1995). The polyclonal activation of T cells in *Ctla4*$^{-/-}$ mice is most likely a result of the dysfunction of T reg cells because immunodeficient mice reconstituted with the mixed BM cells from wild-type and *Ctla4*$^{-/-}$ mice failed to develop the fatal disease of the *Ctla4*$^{-/-}$ mice and the deletion of the CTLA-4 gene in FoxP3$^+$ T reg cells recapitulated the fatal disease of the *Ctla4*$^{-/-}$ mice (Bachmann et al., 1999; Wing et al., 2008). Phenotypes of BALB/c-*Pdcd1*$^{-/-}$*Lag3*$^{aida/aida}$ mice are somehow different from those of *Ctla4*$^{-/-}$ mice. In BALB/c-*Pdcd1*$^{-/-}$*Lag3*$^{aida/aida}$ mice, the increase of splenocytes

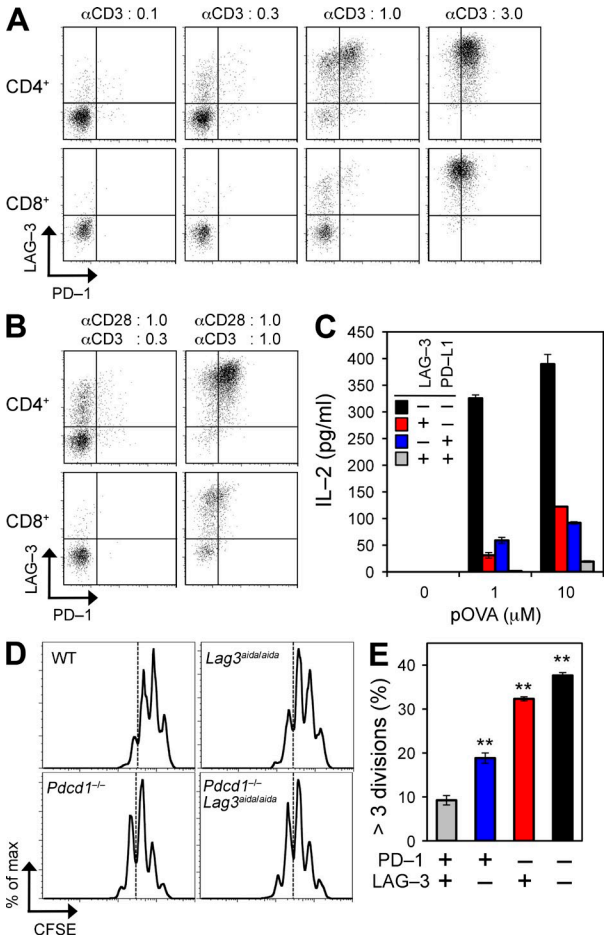

Figure 9. LAG-3 and PD-1 act synergistically to suppress CD4+ T cell activation. (A and B) Splenocytes were stimulated with the indicated concentrations (μg/ml) of plate-bound anti-CD3 Ab in the absence (A) or presence (B) of soluble anti-CD28 Ab for 48 h, and the expression of LAG-3 and PD-1 was analyzed by flow cytometry. Plots are gated on CD4+ or CD8+ cells where indicated. Representative data from two independent experiments are shown. (C) DO11.10 cells transduced or not with LAG-3–expressing retrovirus, were stimulated with OVA peptide–pulsed IIA1.6 cells, transduced or not with PD-L1–expressing retrovirus. T cell IL-2 production was measured by ELISA. Data are the mean ± SEM of duplicate wells. Representative data of two independent experiments are shown. (D and E) Naive CD4+ T cells were sorted from DO11.10 TCR transgenic mice lacking PD-1, LAG-3, or both. Cells were labeled with CFSE and stimulated with IIA1.6–PD-L1 cells pulsed with 0.3 μM OVA peptide. After 2 d, cells were analyzed by flow cytometry. Representative CFSE dilution profiles are shown in D. The frequency of cells with more than three divisions was compared among four genotypes (E). Data are mean ± SEM of triplicate wells. Representative data of two independent experiments are shown. **, $P < 0.01$ compared with the other three groups.

was marginal. T cells were highly activated in heart but their activation was rather modest in spleen compared with *Ctla4*$^{-/-}$ mice. In addition, hearts are preferentially attacked in BALB/c-*Pdcd1*$^{-/-}$*Lag3*$^{aida/aida}$ mice, whereas various organs are affected in *Ctla4*$^{-/-}$ mice. T reg cells from BALB/c-*Pdcd1*$^{-/-}$*Lag3*$^{aida/aida}$ mice had substantial suppressive function and responder cells from BALB/c-*Pdcd1*$^{-/-}$*Lag3*$^{aida/aida}$ were suppressed well by T reg cells in vitro. In addition, immunodeficient mice reconstituted with the mixed BM cells from BALB/c-*Pdcd1*$^{-/-}$*Lag3*$^{aida/aida}$ and wild-type mice developed lethal myocarditis. These results do not support the idea that the main cause of the lethal myocarditis in BALB/c-*Pdcd1*$^{-/-}$*Lag3*$^{aida/aida}$ mice is the failure in regulatory cells by the loss of these negative receptors.

Coexpression of PD-1 and LAG-3 on CD8+ T cells was recently reported by three groups (Blackburn et al., 2009; Grosso et al., 2009; Richter et al., 2010). Blackburn et al. (2009) reported that exhausted CD8+ T cells in a mouse model of chronic lymphocytic choriomeningitis virus (LCMV) infection express seven kinds of inhibitory immunoreceptors, including PD-1 and LAG-3. They also showed that PD-1 blockade partially reverses the exhaustion of CD8+ T cells. Although the effect of LAG-3 blockade alone was marginal, the simultaneous blockade of PD-1 and LAG-3 resulted in a better reversal of exhaustion than the blockade of PD-1 alone. Richter et al. (2010) also reported that LAG-3 is highly expressed on exhausted LCMV-specific CD8+ T cells. However, they reported that chronic LCMV infection of *Lag3*$^{-/-}$ mice led to a comparable degree of T cell exhaustion and to similar virus titers as observed in control mice. Grosso et al. (2009) reported that PD-1 and LAG-3 showed sustained expression on CD8+ T cells after stimulation with tolerizing environment. Although the final effector cells of the myocarditis in BALB/c-*Pdcd1*$^{-/-}$*Lag3*$^{aida/aida}$ mice was CD4+ T cells and not CD8+ T cells, a similar scenario may occur in the current model as well. In fact, we found the coexpression of PD-1 and LAG-3 on both activated CD4+ and CD8+ T cells. We also observed synergistic effects of PD-1 and LAG-3 on the inhibition of T cell activation upon antigen stimulation using T cell lines and primary DO11.10 T cells, suggesting that LAG-3 and PD-1 regulate the activation of CD4+ T cells concurrently. Because heart-infiltrating CD4+ T cells were strongly biased to Th1, these receptors may suppress the Th1 response of CD4+ T cells. Interestingly, LAG-3 induction required a weaker stimulation than PD-1 induction. It is possible that LAG-3 primarily responds to autoimmune stimuli and renders autoreactive T cells unresponsive, whereas PD-1 functions as a fail-safe device that suppresses adversely activated autoreactive T cells. In summary, LAG-3 and PD-1 most likely inhibit the activation and/or expansion of heart-reactive CD4+ T cells to prevent myocarditis in BALB/c mice.

The structure of LAG-3 is quite similar to CD4 and LAG-3 is reported to bind to MHC class II (Baixeras et al., 1992; Huard et al., 1997). We found no detectable changes in the negative selection of super antigen-reactive T cells in *Lag3*$^{aida/aida}$ mice in accordance with the previous description (Miyazaki et al., 1996; Fig. S5), suggesting that LAG-3 deficiency may affect peripheral tolerance rather than central tolerance. In our in vitro experimental system, LAG-3 suppressed antigen stimulation in both CD4-positive and -negative cells, as opposed to a previous study (Workman et al., 2002a), indicating that the inhibitory mechanisms of LAG-3 cannot be totally attributed to the competition for MHC class II binding

with CD4. Because the region in the cytoplasmic tail of LAG-3 that has been reported to be critical for its inhibitory function does not include any well defined signaling motifs (Workman et al., 2002a), LAG-3 may transduce a unique inhibitory signal that has not been characterized yet.

Because isotype-switched and somatically mutated autoAbs are frequently found in human patients and model animals of autoimmune diseases, SHM and CSR are supposed to be essential for the development of these diseases. However, it is still controversial whether the lack of SHM and CSR alleviates autoimmunity or not. Jiang et al. (2007) reported that MRL-*Fas*$^{lpr/lpr}$*Aicda*$^{-/-}$ mice developed much milder glomerulonephritis and survived longer compared with AID-sufficient littermates, indicating that CSR and SHM are essential for the development of glomerulonephritis in MRL-*Fas*$^{lpr/lpr}$ mice. Interestingly, MRL-*Fas*$^{lpr/lpr}$*Aicda*$^{-/-}$ mice produced a five-times-higher amount of anti-dsDNA IgM than AID-sufficient littermates, suggesting that larger amount of unmutated IgM autoAbs cannot compensate for isotype-switched and mutated autoAbs in the development of glomerulonephritis in MRL-*Fas*$^{lpr/lpr}$ mice. On the contrary, Chen et al. (2010) reported that AID deficiency exacerbated glomerulonephritis in C57BL/6-*Fas*$^{lpr/lpr}$ mice, which develop milder phenotypes compared with MRL-*Fas*$^{lpr/lpr}$ mice. In the current study, we found that SHM and/or CSR are required for the development of gastritis and DCM in BALB/c-*Pdcd1*$^{-/-}$ mice in accordance with our previous findings that IgG autoAbs against cardiac troponin I are responsible for the DCM in BALB/c-*Pdcd1*$^{-/-}$ mice and IgG antiparietal cell autoAbs are highly produced in BALB/c-*Pdcd1*$^{-/-}$ mice with gastritis (Okazaki et al., 2003, 2005). Further analyses on BALB/c-*Pdcd1*$^{-/-}$ mice may elucidate the mechanisms of how autoreactive B cells escape from deletion, are activated, undergo SHM and CSR, and eventually induce overt autoimmune diseases by PD-1 deficiency.

In contrast, SHM and CSR were not required for the development of T1DM in NOD-*Lag3*$^{aida/aida}$ mice and myocarditis in BALB/c-*Pdcd1*$^{-/-}$*Lag3*$^{aida/aida}$ mice. Interestingly, B cells themselves were not required for T1DM in NOD-*Lag3*$^{aida/aida}$ mice because they developed T1DM very early in the absence of B cells. NOD-*Aicda*$^{-/-}$ mice apparently developed T1DM more slowly in the absence of B cells. Because the spontaneous dissociation of *Aicda*$^{-}$ and *Lag3*^{aida} occurred in the colony of NOD-μMT-*Aicda*$^{-/-}$ but not NOD-*Aicda*$^{-/-}$ mice, the delay was most likely a result of the emergence of segregants but not of the lack of B cells. It is widely accepted that B cells play critical roles in T1DM of NOD mice because NOD-μMT mice that lack mature B cells have a very low incidence of T1DM and have a delay and reduction in the severity of insulitis (Serreze et al., 1996; Akashi et al., 1997; Yang et al., 1997). Wong et al. (2004) provided direct evidence that the role of B cells in T1DM of NOD mice relates to their function as antigen-presenting cells rather than to the production of autoAbs. They postulated that the antigen-specific antigen presentation by B cells may efficiently stimulate cognate T cells to break self-tolerance. LAG-3–deficient T cells may not require antigen presentation from B cells to induce T1DM because they are readily activated by other types of cells, which are supposed to be less effective in presenting β cell antigens than B cells.

In the current study, we happened to realize that our colony of BALB/c-*Aicda*$^{-/-}$ mice had acquired the loss-of-function mutation in a neighboring gene encoding LAG-3 during the process of backcrossing on BALB/c background. Recently, Hase et al. (2008) reported that BALB/c-*Aicda*$^{-/-}$ mice develop gastritis. In light of the discovery of the *aida* mutation, it is likely that they were observing the effect of the combined deficiency of AID and LAG-3. However, hyperplasia of the ILFs and the increase of germinal center B cells in *Aicda*$^{-/-}$ mice were confirmed to be dependent on AID deficiency.

The difference in the genetic background has substantial effects on various biological activities. Recently, more and more genetically manipulated mice are backcrossed from one strain to other strains to analyze the function of the manipulated genes on different genetic backgrounds. In the course of backcrossing, we may have spontaneous mutations in neighboring genes as we experienced in the current study. The effects of these mutations can be mistakenly interpreted as the effects of manipulated genes because these mutations are strongly linked to manipulated genes. In addition, such a genetic influence does not need to be an acquired mutation; a donor strain–derived polymorphism can also make a strong effect. In fact, we cannot fully exclude the possibility that the enlargement of ILFs in BALB/c-*Aicda*$^{-/-}$*Lag3*$^{aida/aida}$ mice is the result of a CBA-derived polymorphism in the narrow region containing *Lag3* rather than the dysfunction of LAG-3. Current observation represents another caveat for the interpretation of studies using genetically engineered animals with many backcrosses and passages.

In summary, our current findings provide direct evidence that LAG-3 is a critical regulator of autoimmunity and that synergistic actions of LAG-3 and PD-1 are critical for the prevention of autoimmunity. These two receptors therefore represent potential therapeutic targets for autoimmunity, infectious immunity, tumor immunity, and transplantation.

MATERIALS AND METHODS

Animals. BALB/c-*Pdcd1*$^{-/-}$ mice (N14), which were generated by backcrossing BALB/c-*Pdcd1*$^{-/-}$ mice (N10; Nishimura et al., 2001) on BALB/c mice for four generations, were crossed with BALB/c-*Aicda*$^{-/-}$ mice (N10). The BALB/c-*Aicda*$^{-/-}$ mice (N10; Fagarasan et al., 2002) were backcrossed on NOD mice for more than six generations. NOD-μMT and NOD-SCID mice were purchased from The Jackson Laboratory and Japan Clea, respectively. NOD-*Aicda*$^{-/-}$ mice were further backcrossed on NOD mice, and the NOD-*Lag3*$^{aida/aida}$ mice were separated from the NOD-*Aicda*$^{-/-}$*Lag3*$^{aida/aida}$ mice at N14. C57BL/6-*Lag3*$^{-/-}$ mice were provided by D. Vignali (St. Jude Children's Research Hospital, Memphis, TN), C. Benoist, and D. Mathis (Harvard Medical School, Boston, MA; Miyazaki et al., 1996; Workman et al., 2004). C57BL/6-*Lag3*$^{-/-}$ mice were backcrossed on BALB/c mice for three (Fig. 4) and seven (Figs. 7 and 8) generations and on NOD mice for six generations. Genotypes at *Idd1*, *3*, *5*, and *9* were monitored, and those with NOD-derived alleles were selected. DO11.10 TCR transgenic mice were provided by K. Murphy (Washington University School of Medicine, St. Louis, MO) and Y. Wakatsuki

(Kyoto University, Kyoto, Japan; Murphy et al., 1990). All the mouse protocols were approved by the Institute of Laboratory Animals, Graduate School of Medicine, Kyoto University and the Animal Experimentation Committee of the University of Tokushima. The mice were maintained under SPF conditions.

Assessment of T1DM and histological analysis. Urine glucose was monitored every week using Uropiece S (Astellas) and mice were considered diabetic after two consecutive measurements over 100 mg/dl. Mice were sacrificed when they became moribund for the pathological examination of BALB/c-*Pdcd1*$^{-/-}$*Lag3*$^{aida/aida}$ mice, or at 7–8 wk of age for the evaluation of insulitis. Organs were fixed in 10% buffered formalin, processed, and embedded in paraffin. Sections were stained with H&E using standard techniques. Insulitis was scored as described previously (Wang et al., 2005). In brief, periinsulitis, moderate insulitis, and severe insulitis were scored as 1, 2, and 3, respectively. Gastritis was evaluated as described previously (Jiang et al., 2009).

Evaluation of ILF. Small intestines were filled with 10% formalin in PBS for 5 min before being opened longitudinally, as previously described (Oshima et al., 1996). The opened intestines were further fixed with 10% formalin in PBS for >14 h, and the ILFs on the inside of the intestines were observed under a microscope.

SNPs and microsatellite markers. Information on SNPs and microsatellite markers were obtained from Mouse Phenome Database (http://phenome.jax.org/) and the Sloan-Kettering Mouse Project (https://mouse.mskcc.org/), respectively. For SNPs, we synthesized appropriate primer sets (Life Technologies), amplified DNA fragments using PCR (GeneAmp 9700; Life Technologies), and determined their sequence (Genetic Analyzer 3130xl; Life Technologies). For microsatellite markers, we synthesized primer sets, amplified DNA fragments using PCR, and separated on 4% agarose gels.

RFLP. The LAG-3 gene was amplified by PCR using the following primers: 5′-CTGACGGTCAAGAGGTCTCTTAGG-3′ and 5′-CTACACTTCTGGAGGTCCTCAGAC-3′. The PCR fragments were digested with XhoI (Takara Bio Inc.) and separated on 2.5% agarose gels.

Transfer experiments. CD4$^+$ T cells and CD4-depleted splenocytes were prepared from moribund BALB/c-*Pdcd1*$^{-/-}$*Aicda*$^{-/-}$*Lag3*$^{aida/aida}$ mice using anti-CD4 microbeads (Miltenyi Biotec). Unfractionated splenocytes (2×10^7), CD4$^+$ T cells (0.8×10^7, >95% pure and <0.3% contamination of CD8$^+$ T cells on average), or CD4-depleted splenocytes (1.6×10^7, <0.5% contamination of CD4$^+$ T cells on average) were transferred intravenously into 4–6-wk-old BALB/c-*Rag2*$^{-/-}$ mice. BM cells were prepared from 4-wk-old NOD-*Aicda*$^{-/-}$*Lag3*$^{aida/aida}$ or NOD wild-type mice and 1.5×10^7 BM cells were transferred intravenously into sublethally irradiated (3.5 Gy) NOD-SCID or NOD-SCID-*Aicda*$^{-/-}$ mice. We prepared BM cells from mice with indicated genotype and depleted mature CD4$^+$ and CD8$^+$ T cells using magnetic beads (BD; <0.2% and <0.02% contamination of CD4$^+$ and CD8$^+$ T cells, respectively, on average). We transferred 0.5×10^7 BM cells from BALB/c-*Pdcd1*$^{-/-}$*Lag3*$^{aida/aida}$ mice intravenously into sublethally irradiated (3.5 Gy) BALB/c-*Rag2*$^{-/-}$ mice with or without the same number of BM cells from BALB/c wild-type or BALB/c-*Lag3*$^{aida/aida}$ mice. Recipient mice were analyzed 5–7 wk after the transfer.

Flow cytometric analysis. Heart infiltrates were prepared as described previously (Wang et al., 2010). Splenocytes, heart infiltrates, and Peyer's patch cells were stained with the indicated Abs. Data were obtained with FACSCalibur (BD) or Gallios (Beckman Coulter) and analyzed using CellQuest (BD) or FlowJo (Tree Star, Inc.). Cytoplasmic staining was performed as described previously (Wang et al., 2005). In brief, splenocytes and heart infiltrates were stimulated with 10 ng/ml PMA and 1 μg/ml ionomycin for 5 h with Monensin (BioLegend), stained with the indicated Abs, and analyzed by Gallios. Nuclear FoxP3 was detected using a staining kit according to the manufacturer's instruction (BioLegend). Abs against CD28, and Vβs, were purchased from BD, biotin-conjugated PNA was purchased from Vector Laboratories, Abs against LAG-3, IL-4, IFN-γ, Gr1, PD-1, Mac1, and CD62L were purchased from eBioscience, and all the other Abs used in this study were purchased from BioLegend.

Real-time PCR. Total RNA was isolated from spleens of BALB/c wild-type mice and inflamed hearts of BALB/c-*Pdcd1*$^{-/-}$*Lag3*$^{aida/aida}$ mice using TRIzol (Life Technologies) and single-strand cDNA was synthesized using High-Capacity cDNA Reverse Transcription kits according to the manufacturer's instruction (Life Technologies). Gene expression profiling was performed using Taqman Low Density Array Immuno Profiling Plate (Life Technologies) and the comparative cycle threshold (C_t) method as described previously (Wang et al., 2010). The hypoxanthine guanine phosphoribosyl transferase (*Hprt*) was used as an endogenous control and the calibrator samples were spleens of age-matched BALB/c wild-type mice.

In vitro stimulation. Splenocytes were stimulated with plate-bound anti-CD3 Abs (2C11) with or without soluble anti-CD28 Abs at the indicated concentration, and PD-1 and LAG-3 on the surface were detected 1-3 d later. Mouse LAG-3 cDNA was cloned by PCR and introduced into DO11.10 and 2B4.11 cells by retroviral infection. Control vector lacking LAG-3 cDNA was used. Mouse PD-L1 cDNA was cloned by PCR and introduced into IIA1.6 cells, an Fc receptor–negative mouse B cell line. Cognate OVA peptide (ISQAVHAAHAEINEAGR, >95% purity) and cytochrome *c* peptide (ANERADLIAYLKQATK, >95% purity) were synthesized by Sigma-Aldrich. DO11.10 cells with or without LAG-3 (5×10^4 cells/well) were stimulated with peptide-pulsed IIA1.6 cells with or without PD-L1 (10^4 cells/well) for 24 h. The amount of IL-2 in the culture supernatant was quantified by ELISA (BioLegend). BM-derived DCs were generated from C3H/HeN mice (Japan SLC) as described previously (Denda-Nagai et al., 2002) and used for the stimulation of 2B4.11 cells. Primary CD4$^+$ T cells expressing DO11.10 TCR were prepared from mice with indicated genotype. We sorted naive (CD4$^+$CD62L$^+$) cells using MoFlo XDP (Beckman Coulter), labeled with CFSE (Life Technologies), and stimulated with peptide-pulsed IIA1.6-PD-L1 cells treated with mitomycin C (Kyowa Hakko Kirin). We analyzed the dilution of CFSE 2 d later.

In vitro T reg cell assay. The in vitro T reg cell assay was performed as previously described (Sakaguchi et al., 1995; Yoshida et al., 2008). In brief, CD4$^+$CD62L$^+$CD25$^-$ effector T cells and CD4$^+$CD62L$^+$CD25$^+$ T reg cells were prepared from mice with the indicated genotype using MoFlo XDP. T cell–depleted spleen cells from BALB/c wild-type mice were treated with mitomycin C and used as APCs. The purity of the prepared cells was >97%. CFSE-labeled CD25$^-$ effector T cells (2.5×10^4 cells) and 5×10^4 APCs were cultured in 96-well plates for 3 d with 1.0 μg/ml anti-CD3 Ab (2C11). CD25$^+$ T reg cells were added to the culture at the indicated ratio against CD25$^-$ T cells. Suppression efficiency was calculated by dividing the frequency of proliferating cells in the presence of T reg cells by that in the absence of T reg cells.

Statistics. The two-tailed unpaired Student's *t* test was used to evaluate statistical significance.

Online Supplemental Material. Fig. S1 shows the mild lymphocytic infiltration in the stomach, salivary gland, pancreas, lung, and liver in addition to the heart of BALB/c-*Pdcd1*$^{-/-}$*Aicda*$^{-/-}$ mice. Fig. S2 shows the spontaneous generation of germinal centers in BALB/c-*Aicda*$^{-/-}$ but not in BALB/c-*Lag3*$^{aida/aida}$ mice. Fig. S3 shows the protection of BALB/c-*Pdcd1*$^{-/-}$ mice from DCM by AID deficiency. Fig. S4 shows the suppression of IL-2 production by LAG-3 in 2B4.11 cells that express CD4. Fig. S5 shows the normal negative selection of superantigen reactive T cells in BALB/c -*Lag3*$^{-/-}$ and BALB/c-*Lag3*$^{aida/aida}$ mice. Table S1 shows the list of genes in the region between *Aicda* and rs37864878. Table S2 summarizes the responsible genes for each phenotype observed in the current study. Online supplemental material is available at http://www.jem.org/cgi/content/full/jem.20100466/DC1.

We thank Drs. D. Vignali, D. Mathis, C. Benoist, K. Murphy, and Y. Wakatsuki for kindly providing their precious mice and Y. Sakamoto for technical assistance.

This work was supported in part by the Core Research for Evolutional Science and Technology Program of the Japan Science and Technology Agency, Grants-in-Aid from the Ministry of Education, Science, Sports, Culture and Technology of Japan (19689012, 20060012, and 22021030), Kanae Foundation for Life and Socio-Medical Science, and Nakajima Foundation.

The authors declare that they have no competing financial interests.

Submitted: 8 March 2010
Accepted: 13 January 2011

REFERENCES

Akashi, T., S. Nagafuchi, K. Anzai, S. Kondo, D. Kitamura, S. Wakana, J. Ono, M. Kikuchi, Y. Niho, and T. Watanabe. 1997. Direct evidence for the contribution of B cells to the progression of insulitis and the development of diabetes in non-obese diabetic mice. *Int. Immunol.* 9:1159–1164. doi:10.1093/intimm/9.8.1159

Bachmann, M.F., G. Köhler, B. Ecabert, T.W. Mak, and M. Kopf. 1999. Cutting edge: lymphoproliferative disease in the absence of CTLA-4 is not T cell autonomous. *J. Immunol.* 163:1128–1131.

Baixeras, E., B. Huard, C. Miossec, S. Jitsukawa, M. Martin, T. Hercend, C. Auffray, F. Triebel, and D. Piatier-Tonneau. 1992. Characterization of the lymphocyte activation gene 3–encoded protein. A new ligand for human leukocyte antigen class II antigens. *J. Exp. Med.* 176:327–337. doi:10.1084/jem.176.2.327

Blackburn, S.D., H. Shin, W.N. Haining, T. Zou, C.J. Workman, A. Polley, M.R. Betts, G.J. Freeman, D.A. Vignali, and E.J. Wherry. 2009. Coregulation of CD8+ T cell exhaustion by multiple inhibitory receptors during chronic viral infection. *Nat. Immunol.* 10:29–37. doi:10.1038/ni.1679

Brunkow, M.E., E.W. Jeffery, K.A. Hjerrild, B. Paeper, L.B. Clark, S.A. Yasayko, J.E. Wilkinson, D. Galas, S.F. Ziegler, and F. Ramsdell. 2001. Disruption of a new forkhead/winged-helix protein, scurfin, results in the fatal lymphoproliferative disorder of the scurfy mouse. *Nat. Genet.* 27:68–73. doi:10.1038/83784

Chen, L., L. Guo, J. Tian, B. Zheng, and S. Han. 2010. Deficiency in activation-induced cytidine deaminase promotes systemic autoimmunity in lpr mice on a C57BL/6 background. *Clin. Exp. Immunol.* 159:169–175. doi:10.1111/j.1365-2249.2009.04058.x

Denda-Nagai, K., N. Kubota, M. Tsuiji, M. Kamata, and T. Irimura. 2002. Macrophage C-type lectin on bone marrow-derived immature dendritic cells is involved in the internalization of glycosylated antigens. *Glycobiology.* 12:443–450. doi:10.1093/glycob/cwf061

Endo, Y., H. Marusawa, K. Kinoshita, T. Morisawa, T. Sakurai, I.M. Okazaki, K. Watashi, K. Shimotohno, T. Honjo, and T. Chiba. 2007. Expression of activation-induced cytidine deaminase in human hepatocytes via NF-kappaB signaling. *Oncogene.* 26:5587–5595. doi:10.1038/sj.onc.1210344

Fagarasan, S., M. Muramatsu, K. Suzuki, H. Nagaoka, H. Hiai, and T. Honjo. 2002. Critical roles of activation-induced cytidine deaminase in the homeostasis of gut flora. *Science.* 298:1424–1427. doi:10.1126/science.1077336

Fontenot, J.D., M.A. Gavin, and A.Y. Rudensky. 2003. Foxp3 programs the development and function of CD4+CD25+ regulatory T cells. *Nat. Immunol.* 4:330–336. doi:10.1038/ni904

Grosso, J.F., C.C. Kelleher, T.J. Harris, C.H. Maris, E.L. Hipkiss, A. De Marzo, R. Anders, G. Netto, D. Getnet, T.C. Bruno, et al. 2007. LAG-3 regulates CD8+ T cell accumulation and effector function in murine self- and tumor-tolerance systems. *J. Clin. Invest.* 117:3383–3392. doi:10.1172/JCI31184

Grosso, J.F., M.V. Goldberg, D. Getnet, T.C. Bruno, H.R. Yen, K.J. Pyle, E. Hipkiss, D.A. Vignali, D.M. Pardoll, and C.G. Drake. 2009. Functionally distinct LAG-3 and PD-1 subsets on activated and chronically stimulated CD8 T cells. *J. Immunol.* 182:6659–6669. doi:10.4049/jimmunol.0804211

Hannier, S., M. Tournier, G. Bismuth, and F. Triebel. 1998. CD3/TCR complex-associated lymphocyte activation gene-3 molecules inhibit CD3/TCR signaling. *J. Immunol.* 161:4058–4065.

Hase, K., D. Takahashi, M. Ebisawa, S. Kawano, K. Itoh, and H. Ohno. 2008. Activation-induced cytidine deaminase deficiency causes organ-specific autoimmune disease. *PLoS One.* 3:e3033. doi:10.1371/journal.pone.0003033

Honjo, T., K. Kinoshita, and M. Muramatsu. 2002. Molecular mechanism of class switch recombination: linkage with somatic hypermutation. *Annu. Rev. Immunol.* 20:165–196. doi:10.1146/annurev.immunol.20.090501.112049

Hori, S., T. Nomura, and S. Sakaguchi. 2003. Control of regulatory T cell development by the transcription factor Foxp3. *Science.* 299:1057–1061. doi:10.1126/science.1079490

Huang, C.T., C.J. Workman, D. Flies, X. Pan, A.L. Marson, G. Zhou, E.L. Hipkiss, S. Ravi, J. Kowalski, H.I. Levitsky, et al. 2004. Role of LAG-3 in regulatory T cells. *Immunity.* 21:503–513. doi:10.1016/j.immuni.2004.08.010

Huard, B., R. Mastrangeli, P. Prigent, D. Bruniquel, S. Donini, N. El-Tayar, B. Maigret, M. Dréano, and F. Triebel. 1997. Characterization of the major histocompatibility complex class II binding site on LAG-3 protein. *Proc. Natl. Acad. Sci. USA.* 94:5744–5749. doi:10.1073/pnas.94.11.5744

Jiang, C., J. Foley, N. Clayton, G. Kissling, M. Jokinen, R. Herbert, and M. Diaz. 2007. Abrogation of lupus nephritis in activation-induced deaminase-deficient MRL/lpr mice. *J. Immunol.* 178:7422–7431.

Jiang, F., T. Yoshida, F. Nakaki, S. Terawaki, S. Chikuma, Y. Kato, I.M. Okazaki, T. Honjo, and T. Okazaki. 2009. Identification of QTLs that modify peripheral neuropathy in NOD.H2b-Pdcd1-/- mice. *Int. Immunol.* 21:499–509. doi:10.1093/intimm/dxp020

Keir, M.E., M.J. Butte, G.J. Freeman, and A.H. Sharpe. 2008. PD-1 and its ligands in tolerance and immunity. *Annu. Rev. Immunol.* 26:677–704. doi:10.1146/annurev.immunol.26.021607.090331

Khattri, R., T. Cox, S.A. Yasayko, and F. Ramsdell. 2003. An essential role for Scurfin in CD4+CD25+ T regulatory cells. *Nat. Immunol.* 4:337–342. doi:10.1038/ni909

Matsumoto, Y., H. Marusawa, K. Kinoshita, Y. Endo, T. Kou, T. Morisawa, T. Azuma, I.M. Okazaki, T. Honjo, and T. Chiba. 2007. Helicobacter pylori infection triggers aberrant expression of activation-induced cytidine deaminase in gastric epithelium. *Nat. Med.* 13:470–476. doi:10.1038/nm1566

Miyazaki, T., A. Dierich, C. Benoist, and D. Mathis. 1996. Independent modes of natural killing distinguished in mice lacking Lag3. *Science.* 272:405–408. doi:10.1126/science.272.5260.405

Muramatsu, M., V.S. Sankaranand, S. Anant, M. Sugai, K. Kinoshita, N.O. Davidson, and T. Honjo. 1999. Specific expression of activation-induced cytidine deaminase (AID), a novel member of the RNA-editing deaminase family in germinal center B cells. *J. Biol. Chem.* 274:18470–18476. doi:10.1074/jbc.274.26.18470

Muramatsu, M., K. Kinoshita, S. Fagarasan, S. Yamada, Y. Shinkai, and T. Honjo. 2000. Class switch recombination and hypermutation require activation-induced cytidine deaminase (AID), a potential RNA editing enzyme. *Cell.* 102:553–563. doi:10.1016/S0092-8674(00)00078-7

Murphy, K.M., A.B. Heimberger, and D.Y. Loh. 1990. Induction by antigen of intrathymic apoptosis of CD4+CD8+TCRlo thymocytes in vivo. *Science.* 250:1720–1723. doi:10.1126/science.2125367

Nishimura, H., T. Okazaki, Y. Tanaka, K. Nakatani, M. Hara, A. Matsumori, S. Sasayama, A. Mizoguchi, H. Hiai, N. Minato, and T. Honjo. 2001. Autoimmune dilated cardiomyopathy in PD-1 receptor-deficient mice. *Science.* 291:319–322. doi:10.1126/science.291.5502.319

Okazaki, T., and T. Honjo. 2006. The PD-1-PD-L pathway in immunological tolerance. *Trends Immunol.* 27:195–201. doi:10.1016/j.it.2006.02.001

Okazaki, I.M., K. Kinoshita, M. Muramatsu, K. Yoshikawa, and T. Honjo. 2002. The AID enzyme induces class switch recombination in fibroblasts. *Nature.* 416:340–345. doi:10.1038/nature727

Okazaki, T., Y. Tanaka, R. Nishio, T. Mitsuiye, A. Mizoguchi, J. Wang, M. Ishida, H. Hiai, A. Matsumori, N. Minato, and T. Honjo. 2003. Autoantibodies against cardiac troponin I are responsible for dilated cardiomyopathy in PD-1-deficient mice. *Nat. Med.* 9:1477–1483. doi:10.1038/nm955

Okazaki, T., Y. Otaka, J. Wang, H. Hiai, T. Takai, J.V. Ravetch, and T. Honjo. 2005. Hydronephrosis associated with antiurothelial and antinuclear autoantibodies in BALB/c-Fcgr2b$^{-/-}$Pdcd1$^{-/-}$ mice. *J. Exp. Med.* 202:1643–1648. doi:10.1084/jem.20051984

Oshima, M., J.E. Dinchuk, S.L. Kargman, H. Oshima, B. Hancock, E. Kwong, J.M. Trzaskos, J.F. Evans, and M.M. Taketo. 1996. Suppression of intestinal polyposis in Apc delta716 knockout mice by inhibition of cyclooxygenase 2 (COX-2). *Cell.* 87:803–809. doi:10.1016/S0092-8674(00)81988-1

Richter, K., P. Agnellini, and A. Oxenius. 2010. On the role of the inhibitory receptor LAG-3 in acute and chronic LCMV infection. *Int. Immunol.* 22:13–23. doi:10.1093/intimm/dxp107

Sakaguchi, S., N. Sakaguchi, M. Asano, M. Itoh, and M. Toda. 1995. Immunologic self-tolerance maintained by activated T cells expressing IL-2 receptor alpha-chains (CD25). Breakdown of a single mechanism of self-tolerance causes various autoimmune diseases. *J. Immunol.* 155:1151–1164.

Serreze, D.V., H.D. Chapman, D.S. Varnum, M.S. Hanson, P.C. Reifsnyder, S.D. Richard, S.A. Fleming, E.H. Leiter, and L.D. Shultz. 1996. B lymphocytes are essential for the initiation of T cell–mediated autoimmune diabetes: analysis of a new "speed congenic" stock of NOD.*Igμ*^{null} mice. *J. Exp. Med.* 184:2049–2053. doi:10.1084/jem.184.5.2049

Shlomchik, M., M. Mascelli, H. Shan, M.Z. Radic, D. Pisetsky, A. Marshak-Rothstein, and M. Weigert. 1990. Anti-DNA antibodies from autoimmune mice arise by clonal expansion and somatic mutation. *J. Exp. Med.* 171:265–292. doi:10.1084/jem.171.1.265

Stott, D.I., F. Hiepe, M. Hummel, G. Steinhauser, and C. Berek. 1998. Antigen-driven clonal proliferation of B cells within the target tissue of an autoimmune disease. The salivary glands of patients with Sjögren's syndrome. *J. Clin. Invest.* 102:938–946. doi:10.1172/JCI3234

Tivol, E.A., F. Borriello, A.N. Schweitzer, W.P. Lynch, J.A. Bluestone, and A.H. Sharpe. 1995. Loss of CTLA-4 leads to massive lymphoproliferation and fatal multiorgan tissue destruction, revealing a critical negative regulatory role of CTLA-4. *Immunity.* 3:541–547. doi:10.1016/1074-7613(95)90125-6

Triebel, F., S. Jitsukawa, E. Baixeras, S. Roman-Roman, C. Genevee, E. Viegas-Pequignot, and T. Hercend. 1990. LAG-3, a novel lymphocyte activation gene closely related to CD4. *J. Exp. Med.* 171:1393–1405. doi:10.1084/jem.171.5.1393

Tsuji, M., N. Komatsu, S. Kawamoto, K. Suzuki, O. Kanagawa, T. Honjo, S. Hori, and S. Fagarasan. 2009. Preferential generation of follicular B helper T cells from Foxp3+ T cells in gut Peyer's patches. *Science.* 323:1488–1492. doi:10.1126/science.1169152

van Es, J.H., F.H. Gmelig Meyling, W.R. van de Akker, H. Aanstoot, R.H. Derksen, and T. Logtenberg. 1991. Somatic mutations in the variable regions of a human IgG anti–double-stranded DNA autoantibody suggest a role for antigen in the induction of systemic lupus erythematosus. *J. Exp. Med.* 173:461–470. doi:10.1084/jem.173.2.461

Wang, J., T. Yoshida, F. Nakaki, H. Hiai, T. Okazaki, and T. Honjo. 2005. Establishment of NOD-Pdcd1-/- mice as an efficient animal model of type I diabetes. *Proc. Natl. Acad. Sci. USA.* 102:11823–11828. doi:10.1073/pnas.0505497102

Wang, J., I.M. Okazaki, T. Yoshida, S. Chikuma, Y. Kato, F. Nakaki, H. Hiai, T. Honjo, and T. Okazaki. 2010. PD-1 deficiency results in the development of fatal myocarditis in MRL mice. *Int. Immunol.* 22:443–452. doi:10.1093/intimm/dxq026

Waterhouse, P., J.M. Penninger, E. Timms, A. Wakeham, A. Shahinian, K.P. Lee, C.B. Thompson, H. Griesser, and T.W. Mak. 1995. Lymphoproliferative disorders with early lethality in mice deficient in Ctla-4. *Science.* 270:985–988. doi:10.1126/science.270.5238.985

Wing, K., Y. Onishi, P. Prieto-Martin, T. Yamaguchi, M. Miyara, Z. Fehervari, T. Nomura, and S. Sakaguchi. 2008. CTLA-4 control over Foxp3+ regulatory T cell function. *Science.* 322:271–275. doi:10.1126/science.1160062

Wong, F.S., L. Wen, M. Tang, M. Ramanathan, I. Visintin, J. Daugherty, L.G. Hannum, C.A. Janeway Jr., and M.J. Shlomchik. 2004. Investigation of the role of B-cells in type 1 diabetes in the NOD mouse. *Diabetes.* 53:2581–2587. doi:10.2337/diabetes.53.10.2581

Workman, C.J., and D.A. Vignali. 2003. The CD4-related molecule, LAG-3 (CD223), regulates the expansion of activated T cells. *Eur. J. Immunol.* 33:970–979. doi:10.1002/eji.200323382

Workman, C.J., and D.A. Vignali. 2005. Negative regulation of T cell homeostasis by lymphocyte activation gene-3 (CD223). *J. Immunol.* 174:688–695.

Workman, C.J., K.J. Dugger, and D.A. Vignali. 2002a. Cutting edge: molecular analysis of the negative regulatory function of lymphocyte activation gene-3. *J. Immunol.* 169:5392–5395.

Workman, C.J., D.S. Rice, K.J. Dugger, C. Kurschner, and D.A. Vignali. 2002b. Phenotypic analysis of the murine CD4-related glycoprotein, CD223 (LAG-3). *Eur. J. Immunol.* 32:2255–2263. doi:10.1002/1521-4141(200208)32:8<2255::AID-IMMU2255>3.0.CO;2-A

Workman, C.J., L.S. Cauley, I.J. Kim, M.A. Blackman, D.L. Woodland, and D.A. Vignali. 2004. Lymphocyte activation gene-3 (CD223) regulates the size of the expanding T cell population following antigen activation in vivo. *J. Immunol.* 172:5450–5455.

Workman, C.J., Y. Wang, K.C. El Kasmi, D.M. Pardoll, P.J. Murray, C.G. Drake, and D.A. Vignali. 2009. LAG-3 regulates plasmacytoid dendritic cell homeostasis. *J. Immunol.* 182:1885–1891. doi:10.4049/jimmunol.0800185

Yagi, T., T. Tokunaga, Y. Furuta, S. Nada, M. Yoshida, T. Tsukada, Y. Saga, N. Takeda, Y. Ikawa, and S. Aizawa. 1993. A novel ES cell line, TT2, with high germline-differentiating potency. *Anal. Biochem.* 214:70–76. doi:10.1006/abio.1993.1458

Yang, M., B. Charlton, and A.M. Gautam. 1997. Development of insulitis and diabetes in B cell-deficient NOD mice. *J. Autoimmun.* 10:257–260. doi:10.1006/jaut.1997.0128

Yoshida, T., F. Jiang, T. Honjo, and T. Okazaki. 2008. PD-1 deficiency reveals various tissue-specific autoimmunity by H-2b and dose-dependent requirement of H-2g7 for diabetes in NOD mice. *Proc. Natl. Acad. Sci. USA.* 105:3533–3538. doi:10.1073/pnas.0710951105